Quantum scattering and adiabatic channel treatment of the low-energy and low-temperature capture of a rotating quadrupolar molecule by an ion

E. I. Dashevskaya, I. Litvin, E. E. Nikitin, and J. Troe

Citation: The Journal of Chemical Physics **120**, 9989 (2004); doi: 10.1063/1.1724822
View online: http://dx.doi.org/10.1063/1.1724822
View Table of Contents: http://scitation.aip.org/content/aip/journal/jcp/120/21?ver=pdfcov
Published by the AIP Publishing

Quantum scattering and adiabatic channel treatment of the low-energy and low-temperature capture of a rotating quadrupolar molecule by an ion

E. I. Dashevskaya
Department of Chemistry, Technion-Israel Institute of Technology, Haifa, 32000 Israel

I. Litvin and E. E. Nikitin
Department of Chemistry, Technion-Israel Institute of Technology, Haifa, 32000 Israel and Institut für Physikalische Chemie der Universität Göttingen, Tammannstrasse 6, D-37077 Göttingen, Germany

J. Troe[a)]
Institut für Physikalische Chemie der Universität Göttingen, Tammannstrasse 6, D-37077 Göttingen, Germany

(Received 18 September 2003; accepted 8 March 2004)

The capture rate coefficients of homonuclear diatomic molecules (H_2 and N_2) in the rotational state $j=1$ interacting with ions (Ar^+ and He^+) are calculated for low collision energies assuming a long-range anisotropic ion-induced dipole and ion–quadrupole interaction. A comparison of accurate quantum rates with quantum and state-specific classical adiabatic channel approximations shows that the former becomes inappropriate in the case when the cross section is dominated by few partial contributions, while the latter performs better. This unexpected result is related to the fact that the classical adiabatic channel approximation artificially simulates the quantum effects of tunneling and overbarrier reflection as well as the Coriolis coupling and it suppresses too high values of the centrifugal barriers predicted by a quantum adiabatic channel approach. For $H_2(j=1)+Ar^+$ and $N_2(j=1)+He^+$ capture, the rate constants at $T\rightarrow 0$ K are about 3 and 6 times higher than the corresponding values for $H_2(j=0)+Ar^+$ and $N_2(j=0)+He^+$ capture. © *2004 American Institute of Physics.* [DOI: 10.1063/1.1724822]

I. INTRODUCTION

Complex formation (capture) in low-temperature collisions of an ion and a diatomic molecule usually occurs with participation of molecules that occupy only low rotational states. If the temperature T is noticeably lower than B/k_B (B is the rotational constant of the molecule in energy units and k_B is the Boltzmann constant), the largest contribution to the capture rate constant (CRC) comes from the ground rotational state of the diatom. If this state is not degenerate, and if the ion is in a nondegenerate electronic state, the dynamics of the capture assumes a particularly simple form since the interaction between the colliding partners is isotropic. If, in addition, the relative motion can be considered as classical, the calculation of the CRC becomes a standard textbook problem. Recently, the classical results have been extended down to lower temperatures, where the relative motion is quantal.[1]

If the states of the colliding partners are degenerate, the problem of calculating CRC becomes more complicated. An economic approach to attack this problem is the adiabatic channel (AC) approximation which simplifies the dynamical problem by assuming that the projection of the intrinsic angular momenta of the collision partners on the collision axis **R** is conserved throughout of the collision event.[2,3] In what follows we assume that the electronic state of the ion is nondegenerate such that the intrinsic angular momentum is identical to the rotational angular momentum of the diatom (quantum number j). A detailed treatment of state-specific ion–molecule capture within the AC approximation, for ion–quadrupole systems, was presented by Smith and Troe[4] under the condition of classical (Cl) relative motion (we call this AC classical approximation, ACCl) who calculated state-specific low temperature rate constants in the perturbed rotor limit.

In this work we consider the cross section and the rate constant for capture, by an ion, of a homonuclear diatom in the first excited rotational state $j=1$. This problem is of special interest for two reasons: first, it represents the main correction to the capture cross section of ground-rotational state (the more so since the interaction in a system ''ion–diatom with $j>0$'' is of longer range than that for a system ''ion–diatom with $j=0$''), and second, the state $j=1$ is the ground rotational state for a specific total nuclear spin of the diatom. This is the reason why we decided to study in detail the capture dynamics for a system ''ion-homonuclear diatom'' in the state $j=1$ in the energy range between the Bethe–Wigner[5,6] and ACCl regimes. We assume that the rotor state $j=1$ is adiabatically isolated from other rotational states, and we calculate the capture cross section within three different approximations: an accurate quantum treatment, a quantum version of AC (ACQ) and the ACCl approximation. We intend to derive a suitable analytical approximation for the capture cross section similar to that suggested for ion-induced dipole capture in Ref. 1. We have especially considered the two systems, $Ar^+ + H_2$ and $He^+ + N_2$, for which

[a)]Author to whom correspondence should be addressed. Electronic mail: shoff@gwdg.de

ACCl results are available.[4] As in Ref. 3, instead of discussing the energy-dependent capture cross sections σ, we consider the energy-dependent rate coefficients K since the latter show simpler limiting behavior at high and low energies. Then we convert K into the temperature-dependent rate constants $\overline{K}$.

The outline of the presentation is the following. In Sec. II we review the theoretical background for calculating capture cross sections and rate coefficients in different approximations. Section III describes the calculation of accurate and approximate capture probabilities. In Secs. IV and V we present results for quantal and classical rate coefficients. Thermal rate constants are presented in Sec. VI. Secs. VII and VIII contain discussion and conclusion.

II. THEORETICAL BACKGROUND

We consider the collision of a structureless particle A (an atomic ion in a closed state) with a rigid rotor B_2 in the rotational state $j=1$ under the assumption that this state is adiabatically isolated from other states. A complex AB_2 is assumed to be formed when partners approach each other at a certain distance R_c. The dynamics of complex formation is characterized by the wave function which is the solution of the Schrödinger equation describing the coupled translational and rotational motion of the partners. The boundary conditions for the wave function are the incoming plane wave and the outgoing spherical wave at large R, and complete absorption at the surface of the complex. The asymptotics of the wave function furnishes the complex formation (capture) probabilities $P^J_{j,\ell}$ which are labeled by the quantum numbers of the total angular momentum J, the relative angular momentum ℓ and the intrinsic angular momentum j of the diatom. For a rotationally unpolarized molecule, the state-specific complex formation quantum (Q) cross section is given by the standard formula for an inelastic cross section (see, e.g., Ref. 7) in which the absolute values of the squared matrix elements of the scattering matrix are replaced by the capture probabilities,

$$\sigma^{\mathrm{Q}}_j(k)=\frac{\pi}{k^2}\sum_{\ell,J}\frac{2J+1}{2j+1}P^J_{j,\ell}(k). \tag{1}$$

Here k is the wave vector which is related to the collision energy E, the relative velocity ν and the relative linear momentum p as $E=\hbar^2k^2/2\mu=p^2/2\mu=\mu\nu^2/2$ with μ being the reduced mass of the collision partners. Since we are discussing the case $j=1$ the subscript j will be dropped and only replaced by unity where necessary.

Following Ref. 7 we adhere to the convention that the quantum numbers of those dynamical quantities that are conserved during the collision appear as superscripts, while others, corresponding to the asymptotic states, appear as subscripts. A wave function in $j\ell J$ representation possesses a definite parity p which is conserved; however, for a given set $j\ell J$, it is redundant and, therefore, appears in parentheses. Instead of the $j\ell J$ representation, one can also use a $j\tilde{\Omega}J$ representation with $\tilde{\Omega}$ being the quantum number of the projection of **j** onto **R** at $R\to\infty$ (the so-called R-helicity representation). A wave functions in the $j\tilde{\Omega}J$ representation does not possess a definite parity, but it can be made so, if the quantities $\tilde{\Omega}$, are replaced by their absolute values $\Omega=|\tilde{\Omega}|$ and the parity p. Since the transformation $j\ell J\leftrightarrow j\Omega pJ$ is unitary, Eq. (1) can be rewritten as

$$\sigma^{\mathrm{Q}}(k)=\frac{1}{3}\sum_{\Omega,p}\sigma^{\mathrm{Q},p}_{\Omega}(k),$$

with

$$\sigma^{\mathrm{Q},p}_{\Omega}=\frac{\pi}{k^2}\sum_J(2J+1)P^{J,p}_{\Omega}(k). \tag{2}$$

Here $\sigma^{\mathrm{Q},p}_{\Omega}(k)$ are the partial quantum cross sections specified by the asymptotic quantum number Ω and the conserved quantum number p. In our case, there are three different partial cross sections $\sigma^{\mathrm{Q},p}_0$, $\sigma^{\mathrm{Q},p}_1$, $\sigma^{\mathrm{Q},\overline{p}}_1$ where p and $\overline{p}$ are the opposite parities.

In the ACQ version of the capture theory one assumes that the projection quantum number $\tilde{\omega}$ of **j** onto the collision axis remains a good quantum number for arbitrary R and one considers one-dimensional radial motion along effective AC potentials $U^{J,\omega}_{\mathrm{eff}}(R)$. The ACQ version of Eq. (2) reads

$$\sigma^{\mathrm{ACQ}}(k)=\frac{1}{3}\sum_{\tilde{\omega}}\sigma^{\mathrm{ACQ},\tilde{\omega}}(k),$$

with

$$\sigma^{\mathrm{ACQ},\tilde{\omega}}(k)=\frac{\pi}{k^2}\sum_J(2J+1)P^{J,\tilde{\omega}}(k), \tag{3}$$

where $P^{J,\tilde{\omega}}$ are the transmission probabilities through and over the centrifugal barriers of the effective radial potential $U^{J,\omega}_{\mathrm{eff}}(R)$, and $\sigma^{\mathrm{ACQ},\tilde{\omega}}(k)$ are the partial cross sections specified by the assumed conserved quantum number $\tilde{\omega}$. Since in this approximation $P^{J,1}=P^{J,-1}$, there are two different partial cross sections $\sigma^{\mathrm{ACQ},0}$, $\sigma^{\mathrm{ACQ},\pm1}$. Of course, instead of quantum numbers $\tilde{\omega}$, one can label the partial cross sections by quantum numbers ω, p, introducing the cross sections $\sigma^{\mathrm{ACQ},\omega,p}$. Within this nomenclature, one has $\sigma^{\mathrm{ACQ},0}=\sigma^{\mathrm{ACQ},0,p}$, $\sigma^{\mathrm{ACQ},\pm1}=\sigma^{\mathrm{ACQ},1,p}=\sigma^{\mathrm{ACQ},1,\overline{p}}$. Though asymptotically $\Omega=\omega$, the cross sections $\sigma^{\mathrm{ACQ},\omega,p}(k)$ and $\sigma^{\mathrm{Q},p}_{\Omega}(k)|_{\Omega=\omega}$ are not equal to each other since the AC approximation does not account for the rotational asymptotic coupling between different ω AC states.[8] Nonetheless, the ACQ cross section $\sigma^{\mathrm{ACQ}}(k)$ is expected to provide a good approximation to the accurate quantum cross section $\sigma^{\mathrm{Q}}(k)$ if the region of rotational coupling lies substantially outside centrifugal barriers.[8]

Finally, the ACCl counterpart of the quantum cross section can be presented as an integral over J of the classical capture probabilities $P^{\omega}(k,J)$,

$$\sigma^{\mathrm{ACCl}}(k)=\frac{1}{3}\sum_{\tilde{\omega}}\sigma^{\mathrm{ACCl},\tilde{\omega}}(k),$$

$$\sigma^{\mathrm{ACCl},\tilde{\omega}}(k)=\frac{\pi}{k^2}\int P^{\omega}(k,J)2J\,dJ. \tag{4}$$

This nomenclature Q and ACCl corresponds to the nomenclature Q and Cl in Ref. 1, where only one adiabatic (i.e., AC) potential was considered.

The state-specific quantum cross sections for capture leads to the energy-dependent state specific rate coefficients

$K^{Q}(E)$ and the temperature-dependent specific rate constants $\overline{K^{Q}}(T)$ which are related to the cross sections $\sigma^{Q}(k)$ in a standard way,

$$K^{Q}(E)=\nu\sigma^{Q}(k), \quad \overline{K^{Q}}(T)=\langle K^{Q}(E)\rangle_{T}, \tag{5}$$

where $\langle\cdots\rangle_{T}$ denotes averaging over the Maxwell–Boltzmann distribution in relative velocities at translational temperature T.

In the following it is expedient to introduce the scaled interparticle distance $\rho=R/R^{*}$ and the scaled wave vector $\kappa=kR^{*}$ with R^{*} to be defined by convenience. In addition, we use, instead of the $K(k)$, a dimensionless rate coefficient $\chi(\kappa)$. We relate the latter to $K(k)$ as

$$K^{Q}(k)=\left(2\pi R^{*}\frac{\hbar}{\mu}\right)\chi^{Q}(\kappa), \tag{6}$$

where $\chi^{Q}(\kappa)$ assumes the form

$$\chi^{Q}(\kappa)=\frac{1}{3}\sum_{\Omega,p,}\chi_{\Omega}^{Q,p}(\kappa),$$

with

$$\chi_{\Omega}^{Q,p}(\kappa)=\frac{1}{2\kappa}\sum_{J=0}^{\infty}(2J+1)P_{\Omega}^{J,p}(\kappa). \tag{7}$$

The ACQ and ACCl counterparts of Eqs. (5)–(7) are defined similarly.

For a pure isotropic interaction, after simple algebra of angular momentum addition, this expression reduces to a formula for the rate coefficient for the isotropic capture,

$$\chi^{Q,\mathrm{iso}}(\kappa)=\frac{1}{2\kappa}\sum_{\ell}(2\ell+1)P^{\ell}(\kappa) \tag{8}$$

which, of course, is valid for any value of j. This formula with $j=0$ in Ref. 1 was used for discussion of rate coefficients over wide energy ranges. Note that the normalization of $\chi^{Q,\mathrm{iso}}$ is chosen in such a way that, with an ion-induced dipole interaction, $U^{\mathrm{Lang}}(R)=-C/R^{4}$ and $R^{*}\equiv R^{\mathrm{Lang}}=\sqrt{2\mu C}/\hbar$, the high-energy Langevin limit of $\chi^{Q,\mathrm{iso}}$ is equal to unity,[1]

$$\chi^{Q,\mathrm{iso}}(\kappa)\big|_{\kappa\gg 1}\equiv\chi^{\mathrm{Lang}}=1. \tag{9}$$

III. RELATIONS FOR ACCURATE AND APPROXIMATE CAPTURE PROBABILITIES

A. Accurate treatment

The scattering wave function can be written in different representations. In order to achieve a simple relation within the AC approach, for the wave functions of the relative motion we use the AC angular basis. The radial parts of these functions are $\psi_{\omega}^{J,p}(R)$ with $\omega=0,1$ and p assuming two different values for two $\omega=1$ states. For simplicity, we rewrite the three functions as $\psi_{0}^{J}\equiv\psi_{0}^{J,p}$, $\psi_{1}^{J}=\psi_{1}^{J,p}$, $\psi_{\overline{1}}^{J}=\psi_{1}^{J,\overline{p}}$ where p and $\overline{p}$ are opposite parities. As described in Ref. 7 and discussed in Ref. 9, ψ_{0}^{J} and ψ_{1}^{J} are coupled by Coriolis interaction, while $\psi_{\overline{1}}^{J}$ satisfies a single equation. Inputs into these equations are the effective AC potentials $v_{\omega}^{J,\mathrm{eff}}$ (channel potentials plus the centrifugal term) and the Coriolis coupling v_{01}^{J}.

The scattering equations should be solved with absorbing boundary conditions on the surface of the complex. In general, this can be done by introducing a negative imaginary potential in the complex region. There exists, however, an alternative approach if the motion of partners approaching the surface of the complex is quasiclassical. Since any quasiclassical functions can be represented as a superposition of incoming and outgoing waves, the absorbing boundary condition corresponds to the quasiclassical functions that contain only the incoming parts of the waves just before they reach the complex surface. Of course, at large distances, the complex-forming multichannel wave function conforms to standard boundary conditions: outgoing waves in all the channels and an incoming wave in a single state with ω, $p=\Omega$, p. In this way, we get three capture probabilities $P_{\Omega}^{J,p}=P_{0}^{J}$, P_{1}^{J}, $P_{\overline{1}}^{J}$. We note in passing that the above boundary conditions close to the surface of the complex are identical to those used in the theory of electron attachment to molecules in the framework of the so-called extended Vogt–Wannier theory (see Ref. 10 and a review paper[11]).

In what follows, we assume that the capture is determined by a special type of long-range anisotropic interaction, i.e., by an anisotropic ion-induced dipole interaction and ion–quadrupole interaction

$$V(R,\gamma)=-\frac{q^{2}\alpha}{2R^{4}}+\left(-\frac{q^{2}\Delta\alpha}{3R^{4}}+\frac{qQ}{R^{3}}\right)\frac{(3\cos^{2}\gamma-1)}{2}, \tag{10}$$

where q is the charge of the ion, α is the mean polarizability, $\alpha=(\alpha_{\parallel}+2\alpha_{\perp})/3$, $\Delta\alpha=\alpha_{\parallel}-\alpha_{\perp}$, and Q is the quadrupole moment of the molecule. The AC quantum numbers $\tilde{\omega}$ and states $|\tilde{\omega}\rangle$ are defined as the result of a diagonalization of the interaction matrix with the quantization axis taken to be the collision axis **R**. In the perturbed rotor approximation, for $j=1$, Eq. (10) generates the following AC potentials:[4]

$$V_{\omega}(R)=-\frac{q^{2}\alpha}{2R^{4}}+\left(-\frac{q^{2}\Delta\alpha}{15R^{4}}+\frac{qQ}{5R^{3}}\right)(2-3\omega^{2}). \tag{11}$$

The AC states are coupled by the rotational coupling; the latter is simplified when one passes from the $\tilde{\omega}$ representation to the ω, p representation. Let us define states $|0\rangle,|1\rangle,|\overline{1}\rangle$ as those corresponding to the states $|0,p\rangle$, $|1,p\rangle$, $|1,\overline{p}\rangle$. Then the Coriolis interaction couples the states $|0\rangle$ and $|1\rangle$, while the state $|\overline{1}\rangle$ remains uncoupled. We now choose the length unit $R^{*}\equiv R_{L}=\sqrt{\mu q^{2}\alpha}/\hbar$ and introduce the energy unit $E^{*}=\hbar^{2}/\mu R_{L}^{2}$. Passing to the dimensionless scaled AC potentials $v_{\omega}=V_{\omega}/E^{*}$, we write the following expressions for the effective AC potentials and the Coriolis interaction:

$$v_{0}^{J,\mathrm{AC,eff}}(\rho)=\frac{(J(J+1)+2)}{2\rho^{2}}-\frac{1}{2\rho^{4}}+\left(\frac{a}{\rho^{4}}+\frac{b}{\rho^{3}}\right),$$

$$v_{1}^{J,\mathrm{AC,eff}}(\rho)=v_{\overline{1}}^{J}(\rho)=\frac{J(J+1)}{2\rho^{2}}-\frac{1}{2\rho^{4}}-\frac{1}{2}\left(\frac{a}{\rho^{4}}+\frac{b}{\rho^{3}}\right),$$

$$v_{10}^{J,\mathrm{AC,Cor}}(\rho)=v_{01}^{J,\mathrm{AC,Cor}}(\rho)=\frac{\sqrt{J(J+1)}}{\rho^{2}}. \tag{12}$$

The single effective AC potential for $J=0$ is

$$v_0^{0,\mathrm{AC,eff}}(\rho)=v_0^{J,\mathrm{AC,eff}}(\rho)|_{J=0}=\frac{1}{\rho^2}-\frac{1}{2\rho^4}+\frac{a}{\rho^4}+\frac{b}{\rho^3}, \tag{13}$$

where $a=2\Delta\alpha/15\alpha$, $b=2\mu qQ/5R_L\hbar^2$. Here one term, v^{iso}, is the scaled isotropic ion-induced dipole interaction. The other term, $v_\omega^{\mathrm{aniso}}$, contains two interaction parameters: parameter a encompasses the scaled anisotropic ion-induced dipole interaction and the parameter b results from first-order ion–quadrupole interaction. The values of these parameters for the two systems considered are listed in Table I.

If a is zero or very small (such as this is the case here), the potential v_1 is attractive, and potential v_0 at large distances is repulsive for the case $b>0$, while the potential v_0 at large distances is attractive and v_1 is initially repulsive for the case $b<0$. These two cases are called conventionally the even and odd cases, see Ref. 4. In this paper we only consider the collision energies that are noticeably below the potential barriers for v_0 [in the even case, $v_0^{\max}=(1/6)(3b/2)^4=0.84b^4$] and for v_1 [in the odd case, $v_1^{\max}=(1/6)(3b/4)^4=0.05b^4$], and, therefore, we will regard the at large distances repulsive potentials as purely repulsive. Note that all the effective AC potentials are repulsive at large distances.

B. AC calculations

Within the standard AC approximation, the rotational coupling is neglected completely such that the AC capture probabilities $P^{J,\tilde{\omega}}$ are simply the transmission probabilities through the centrifugal barriers of the effective potentials $v_\omega^{J,\mathrm{AC,eff}}$. The transmission probabilities are found from the respective AC wave functions $\psi^{\mathrm{AC},J,\tilde{\omega}}$ that satisfy the uncoupled scattering equations similar to those of Ref. 1.

C. ACCl calculations

Within the ACCl approximation, the transition probabilities $P^{\tilde{\omega}}(\kappa,J)$ are Heaviside step functions,

$$P^{\tilde{\omega}}(\kappa,J)=\begin{cases}\Theta\left[\dfrac{\kappa^2}{2}-\max(v_\omega^{J,\mathrm{AC,eff}}(\rho))\right], & \text{for attractive AC potentials,}\\ 0, & \text{for repulsive AC potentials,}\end{cases} \tag{14}$$

where $\Theta(x)$ is the Heaviside step function. Note that for the even case $\omega=1$, and for the odd case $\omega=0$.

IV. CLASSICAL AC RATE COEFFICIENTS

The capture rate coefficient within the ACCl approach reads

$$\chi^{\mathrm{ACCl}}(\kappa)=\frac{1}{6\kappa}\begin{cases}J_0^2(\kappa), & \text{for attractive AC potentials with } \tilde{\omega}=0, \text{ in the odd case,}\\ 2J_1^2(\kappa), & \text{for attractive AC potentials with } \tilde{\omega}=\pm 1, \text{ in the even case,}\end{cases} \tag{15}$$

where the $J_\omega(\kappa)$ are found from the solutions of the equation

$$\max\{v_\omega^{J,\mathrm{AC,eff}}(\rho)|_{J=J_\omega}\}=\frac{\kappa^2}{2} \tag{16}$$

with $\omega=0$, for the odd case, and $\omega=1$, for the even case.

One can express quasiclassical AC rate coefficients through the rate coefficients for a certain reference potential $V_r(R)$, provided that the latter has a structure similar to that for AC potentials. For this purpose we consider the classical capture in the field of a certain potential $V_r(R)$. The standard equations for the capture yield the angular momentum for the orbiting trajectory, M_c, as a function of the initial linear momentum of relative motion, P. In terms of these quantities, the capture cross section S_r and the capture rate coefficient K_r for the reference potential are

$$S_r=\pi\frac{M_c^2}{P^2},\quad K_r=\frac{\pi}{\mu}\frac{M_c^2}{P}. \tag{17}$$

The calculation of S_r and K_r can be simplified if one introduces scaling parameters, a unit of length R_0 and a unit of action A. Then the initial variables R, P, M_c can be expressed via the scaled dimensionless variables r, p, m_c as

$$r=R/R_0,\quad p=PR_0/A,\quad m_c=M_c/A. \tag{18}$$

With this scaling, the unit of energy is $E_0=A^2/\mu R_0^2$, and the dimensionless energy is $\varepsilon=E/E_0$. We then introduce the reduced rate coefficient $X_r(p)=m_c^2(p)/2p$ which is related to K_r as

$$K_r=\frac{2\pi AR_0}{\mu}X_r(p). \tag{19}$$

Up to this point, the two parameters R_0 and A remained arbitrary and they could be defined as a matter of convenience. We consider two possible choices.

(i) R_0 and A can be chosen in order to decrease the number of parameters entering into the potential $V_r(R)$ by two. For the interaction containing two inverse-power terms (such as $-C_4/R^4$ and $-C_3/R^3$), the scaled potential $\nu(r)$ can be written in a the form $\nu(r)=-1/2r^4-1/2r^3$. The function $X_r(r_c)$ in Eq. (19) will contain no parameters. The scaling parameters do appear, however, when one passes to the rate coefficient K_r and when one expresses the collision energy E through dimensionless energy ε. This choice of parameters was also adopted in Ref. 4 where the ratio of the thermally averaged classical capture rate to the Langevin

capture rate was discussed (see Fig. 4 in Ref. 4). However, this choice appears inconvenient when the relation between classical and quantum rates is discussed.

(ii) R_0 and A can be chosen in order to provide a quasiclassical correspondence between the classical angular momentum M and its quantum number counterpart ℓ, i.e., $A=\hbar$; R_0 can be chosen in such a way that the isotropic part of the ion-induced dipole term in the AC potential takes the form $-1/2r^4$. With this choice of R_0 and A, the dimensionless distance r coincides with ρ, the dimensionless linear momentum p coincides with κ, and the classical function $X_r=X_r(p)$ represents the quasiclassical counterpart of the AC quantum function $\chi^{\mathrm{ACQ}}=\chi_r^{\mathrm{ACQ}}(\kappa)$ for the AC potential which coincides with the reference potential. In other words, $X_r(p)\equiv\chi_r^{\mathrm{ACCl}}(\kappa)$. Of course, in this case $X_r(p)$ and $\chi_r^{\mathrm{ACCl}}(\kappa)$ depend additionally on the parameters that enter into the reference and AC potentials, respectively.

For our purpose, instead of plotting $\chi_r^{\mathrm{ACCl}}(\kappa)$ as a function of the wave vector κ, it is more instructive to plot χ_r^{ACCl} as a function of the properly defined scaled capture angular momentum λ. In accord with Ref. 1, the latter is defined in such a way that it becomes equal to the angular momentum quantum number ℓ whenever the collision energy becomes equal to the height of centrifugal barrier for a given value of ℓ. In other words, integer values of $\lambda=0,1,2,...$, correspond to the collision energies at which the capture channels with $\ell=0,1,2,...$, become classically open. The representation in terms of a variable λ prepares the ground for a discussion of quantum effects, which are expected to show up within the energy range corresponding to low λ.

We define λ through m_c as

$$\lambda=\sqrt{m_c^2+1/4}-1/2=\sqrt{2\kappa X_r+1/4}-1/2. \tag{20}$$

The function λ has the desired property, viz. $\lambda(\lambda+1)=m_c^2$ with m_c^2 being the reduced capture orbital momentum.

As an example, we take as $\nu_r(r)$ an isotropic ion-induced dipole plus ion–quadrupole potential [potentials from Eq. (12) with $a=0$]. For this case, we have the following expressions for the ACCl rate coefficients for the cases $b>0$ and $b<0$:

$$\chi_{\mathrm{even}}^{\mathrm{ACCl}}=\frac{2}{3}X_b,\quad \nu_b(r)=-\frac{1}{r^4}-\frac{b}{2r^3},\quad b>0, \tag{21a}$$

$$\chi_{\mathrm{odd}}^{\mathrm{ACCl}}=\frac{1}{3}X_b,\quad \nu_b(r)=-\frac{1}{2r^4}+\frac{b}{r^3},\quad b<0. \tag{21b}$$

The asymptotic forms of X_b for small and large κ are

$$X_b|_{b>0}=\begin{cases}\dfrac{3\times 2^{1/3}}{4}\left(\dfrac{b^2}{\kappa}\right)^{1/3} & \text{for } \kappa\ll b^2,\\ 1 \quad \text{for } \kappa\gg b^2,\end{cases} \tag{22a}$$

$$X_b|_{b<0}=\begin{cases}\dfrac{3\times 2^{1/3}}{4}\left(\dfrac{4b^2}{\kappa}\right)^{1/3} & \text{for } \kappa\ll b^2,\\ 1 \quad \text{for } \kappa\gg b^2.\end{cases} \tag{22b}$$

Plots of λ_b versus κ and X_b versus λ_b are presented in Figs. 1 and 2, for b ranging from 2.5 to 20. The blank area for $\lambda<1$ is the region where the quasiclassical approximation is expected to break down completely. The aim of the quantal calculations of the rate coefficients is to cover this region and to elucidate the convergence of χ^{Q} and χ^{ACQ} to χ^{ACCl} for $\lambda>1$. We note in passing that, if we extrapolate the expression for X_b down to the boundary of the quantum region, say to $\lambda_b=1$, we get $X_b|_{\lambda_b\approx 1}\propto b$ for sufficiently large b. Since, according to the Bethe law, the quantum rate coefficient has a finite value in the limit $\lambda_b\ll 1$, the above result suggests that the zero-energy quantum rate coefficient is proportional to b. We will see in Sec. V that this is indeed the case.

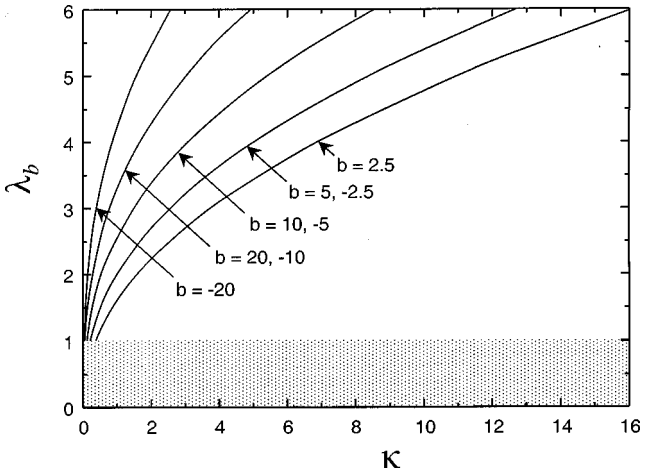

FIG. 1. Plots of λ_b vs κ for the reference potentials of Eq. (21) and selected values of the parameter b. In the region $\lambda\leqslant 1$, the classical description is certainly not valid.

In Fig. 2, along with the rate coefficients X_b for the ion-induced dipole+ion–quadrupole interaction of Eq. (30), we show also the asymptotic rate coefficients X_b^{as} from Eq. (30) which correspond to pure ion–quadrupole interaction for two cases, $b=5$ and $b=-10$. We see that X_b and X_b^{as} coalesce for small λ; this is expected since, at low energies, the main contribution to the capture comes from the long-range part of the potential. But we see also that this coalescence for $b=5$ occurs only in the quantal region. Since the

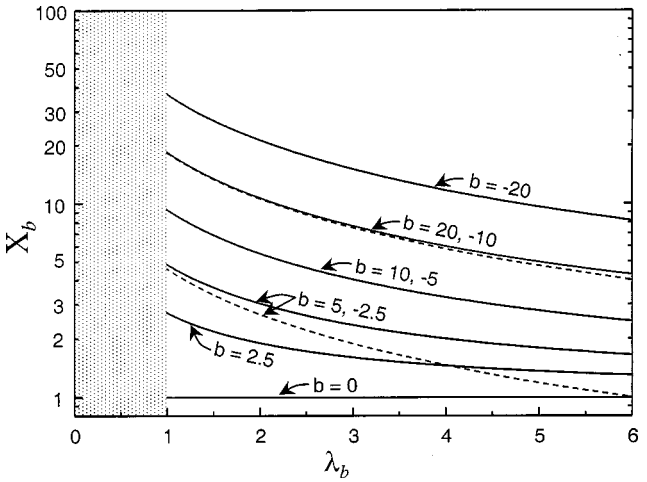

FIG. 2. Reference capture rate coefficients X_b vs λ_b (full lines) for selected values of the parameter b. The dotted lines correspond to the rate coefficients for pure ion–quadrupole interaction. In the region $\lambda\leqslant 1$, the classical description is certainly not valid.

TABLE I. Interaction parameters for the H_2+Ar^+ and N_2+He^+ systems (from the values of α, $\Delta\alpha$, and Q used in Ref. 4).

System	α, a.u.	$\Delta\alpha$, a.u.	Q, a.u.	R_L, a.u.	a	b
H_2+Ar^+	5.437	2.12	0.474	138	−0,052	4.81
N_2+He^+	11.74	4.79	−1.09	274	−0.0545	−10.2

value of b for H_2-Ar^+ interaction is close to 5, we expect that, assuming the pure ion–quadrupole interaction, there does not exist an energy range where H_2-Ar^+ capture can be described classically.

V. RESULTS FOR ACCURATE QUANTUM, ACQ, AND ACCI RATE COEFFICIENTS

Calculations of $\chi^{Q}(\kappa)$, and $\chi^{ACQ}(\kappa)$ were done by solving the coupled and uncoupled Schrödinger equations, respectively, for the two collision processes H_2+Ar^+ and N_2+He^+. The interaction parameters for these systems are listed in Table I, and the rate coefficients are presented in Figs. 3 and 4. Shown are the three rate coefficients $\chi^{Q}(\kappa)$, $\chi^{ACQ}(\kappa)$, and $\chi^{ACCl}(\kappa)$ versus the variable $\lambda(\kappa)$ which is defined as a solution to the capture equation;

$$\max\left\{\frac{\lambda(\lambda+1)}{2\rho^2}+v_{\omega}^{AC}(\rho)\right\}=\frac{\kappa^2}{2}, \tag{23}$$

with $\omega=1$ for the even case (H_2+Ar^+ capture) and $\omega=0$ for the odd case (N_2+He^+ capture). The following aspects of Figs. 3 and 4 deserve particular attention.

High energy limit: The high-energy limit $\kappa\gg1$ corresponds to large $\lambda\gg1$, when many capture channels are classically open. Here, all three rate coefficients $\chi^{Q}(\kappa)$, $\chi^{ACQ}(\kappa)$, and $\chi^{ACCl}(\kappa)$ are close to each other. Except for small-amplitude undulations of $\chi^{Q}(\kappa)$ and $\chi^{ACQ}(\kappa)$, which are due to the successive opening of new capture channels, this is expected. In the limit of high energy, the capture event is dominated by the ion-induced dipole interaction. Since the polarization anisotropy in both cases is very small ($a\ll1$),

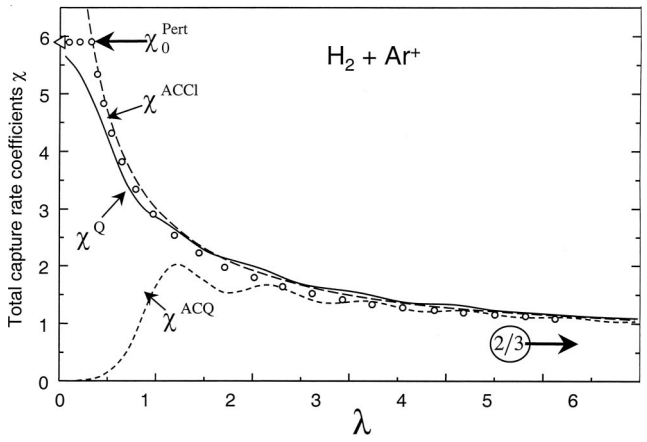

FIG. 3. $H_2(j=1)+Ar^+$ capture. Accurate quantum, χ^{Q} (full line), adiabatic channel quantum, χ^{ACQ} (short dashed line), and adiabatic channel classical, χ^{ACCI} (long dashed line), reduced energy-dependent rate coefficients vs "classical angular momentum quantum number" λ. Left and right arrows indicate approximate zero-energy and exact high-energy limits of χ^{Q}. Open circles correspond to the approximation in Eq. (30).

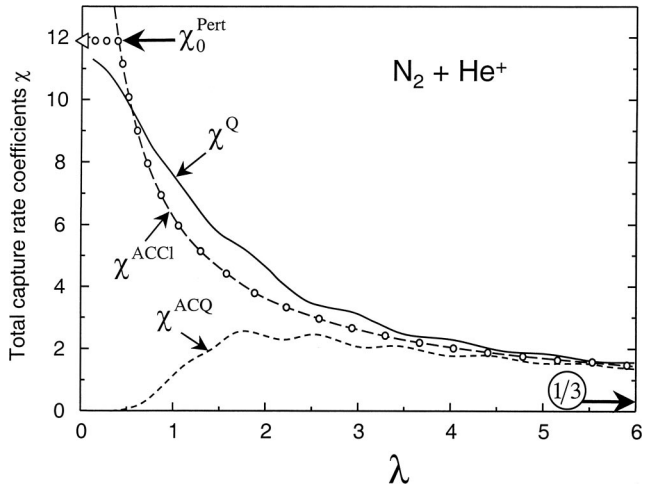

FIG. 4. As in Fig. 3 but for $N_2(j=1)+He^+$ capture.

the high-energy limit of the capture rate coefficients is the Langevin expression. With our choice of the length unit, we get $\chi^{Q}_{\lambda\gg1}$, $\chi^{ACQ}_{\lambda\gg1}\rightarrow\chi^{ACCl}\rightarrow\chi^{Lang}=1$.

Low-energy limit: The low-energy limit $\kappa\ll1$ corresponds to $\lambda\ll1$ when the rate constant is determined by the contribution of terms with small angular momenta only.

(i) The ACCl rate coefficient shows the familiar behavior: it diverges as $\kappa^{-1/3}$, similar to that of a capture rate coefficient for an isotropic attractive interaction proportional to $-1/R^3$. This behavior is in conflict with the Bethe law.[12]

(ii) The ACQ rate coefficient tends to zero in the limit $\kappa\rightarrow0$. This is in accord with the Wigner threshold law.[12] Indeed, in the field of an attractive potential the partial capture rate coefficient for small κ in the channel with angular momentum ℓ is proportional to $\kappa^{2\ell}$. The lowest attractive AC potential in Eq. (12) corresponds to $J=\omega=1$ so that for small κ, $\chi^{ACQ}(\kappa)\approx\chi^{ACQ,1}(\kappa)\propto\kappa^2$. However, this conclusion is not in accord with the Bethe law, which predicts a final, nonzero value of the rate coefficient in the limit $\kappa\rightarrow0$. This incorrect result is due to the neglect of nonadiabatic effects, which, as we shall see, play a decisive part in the low-energy capture dynamics.

(iii) The accurate quantum rate constants conform with the Bethe law. In order to understand the limiting values of $\chi^{Q}(\kappa)$, $\chi^{Q}_0=\chi^{Q}(\kappa)|_{\kappa=0}=\chi^{Q,1}(\kappa)|_{\kappa=0}$, it appears desirable to formulate an approximate scheme that would yield an approximate value of χ^{Q}_0. Since the Coriolis coupling plays a dominant part in the capture dynamics, one can attempt to formulate a perturbation scheme in which the Coriolis interaction is considered in zero order, while the interfragment interaction is regarded as a perturbation. This is easily done since our problem corresponds to the case of an atomic collision between an ion A^+ and an atom B in a state $j=1$. In this spirit, the AC approximation for the ion–molecule case corresponds to the Hund coupling case *b* of a diatom, while the perturbation approach, which we are looking for, corresponds to the Hund coupling case *d*. The switching between different Hund coupling cases is well developed,[7,13] so that one can use a standard technique in calculating the interaction. In the Hund coupling case *d*, the good quantum num-

bers are the orbital momentum quantum number ℓ and the quantum number of the intrinsic angular momentum j. In discussing the zero-energy limit of the rate coefficient, we are interested in the state $\ell=0$ which does not produce a centrifugal barrier. In the zero and first order, the interfragment interaction is equal to the isotropic potential. In our case, this is the isotropic ion-induced dipole interaction proportional to R^{-4}. The anisotropic part of the potential shows up only in the second order. In our case, the anisotropic part of the potential is mainly the ion–quadrupole interaction (note that a is very small) such that the second-order interaction is proportional to the square of the anisotropic part of the interaction, $(R^{-3})^2$, divided by the zero-order energy difference of the two coupled states, $\ell=0$ and $\ell'=2$. This difference is just the difference in the rotational energies of the pair for two values of ℓ, which is proportional to R^{-2}. In this way, the second order correction to the isotropic interaction turns out to be proportional to R^{-4}. In other words, the interaction energy in the channel with $\ell=0$ becomes a modified ion-induced dipole interaction, and, therefore, the results of our previous analysis[1] for s-wave capture become applicable. The explicit calculation then yield the following expression for the interaction potential $v^{\mathrm{pert}}(\rho)$ within the perturbative approach:

$$v^{\mathrm{pert}}(\rho)=-\frac{1}{2\rho^4}(1+b^2/3). \tag{24}$$

Let $P^{\mathrm{pert}}(\kappa)$ be the capture probability for the potential v^{pert} from Eq. (24) in the limit of small κ. Then

$$\chi_0^{\mathrm{Q}}=\chi_0^{\mathrm{Q},1}\approx\chi_0^{\mathrm{pert}}=\lim_{\kappa\to 0}\frac{2J+1}{6\kappa}P^{\mathrm{pert}}(\kappa)\bigg|_{J=1}. \tag{25}$$

For small κ, P^{pert} is linear in κ, and reads $P^{\mathrm{pert}}=4\kappa\sqrt{1+b^2/3}$.[1] Thus we get

$$\chi_0^{\mathrm{pert}}=2\sqrt{1+b^2/3}. \tag{26}$$

For the considered two capture processes H_2+Ar^+ and N_2+He^+, we find $\chi_0^{\mathrm{pert}}=5.90$ and $\chi_0^{\mathrm{pert}}=11.95$, respectively. These numbers are presented by heavy dots in Fig. 3 and Fig. 4. We indeed see that a perturbative treatment explains the accurate numerical results in the zero-energy limit.

Intermediate energies: In the intermediate energy regime $(1\leqslant\lambda\leqslant 4)$ two features deserve discussion: the relation between χ^{Q}, χ^{ACQ}, and χ^{ACCl} for each of the collision events, and the difference between the capture rates for two processes.

(i) For both H_2+Ar^+ and N_2+He^+ collisions the AC classical approach, χ^{ACCl}, approximates the accurate rate coefficients χ^{Q} better than the AC quantum approach does. Since we know[1] that the classical approximation, by replacing the sum over angular momenta with an integral, quite well simulates the quantum effects of tunneling and overbarrier reflections, the noticeable difference between χ^{ACCl} and χ^{ACQ} with a smaller difference between χ^{ACCl} and χ^{Q} should be ascribed to yet another effect that partly simulates the nonadiabatic coupling within the ACCl approach: a partial decrease of the height of the ACClI centrifugal barrier potential compared to ACQ barrier height. This follows from the simple observation that the expectation value of the square of the orbital angular momentum operator conforms to the following relation: $\langle\hat{\mathbf{I}}^2\rangle_J^{\mathrm{ACQ}}\geqslant\langle\mathbf{I}^2\rangle_J^{\mathrm{ACCl}}=J^2$. We thus see that an *ad hoc* replacement of the expectation value of the square of the orbital angular momentum by J^2 in the ACCl approach slightly suppresses centrifugal barriers and thus increases the capture rate. Presumably, this effect can be described more consistently within the so-called axially nonadiabatic channel approach.[14]

(ii) The classical approximation works much better for H_2+Ar^+ than for N_2+He^+. The difference between these two events is that, for the former, the effective potential for the channel with $J=0$ is purely repulsive (b is positive), while, for the latter, it possesses a centrifugal barrier and then becomes attractive (b is negative). Indeed, if the contribution of $\chi^{\mathrm{Q},J}|_{J=0}$ into χ^{Q} is artificially ignored, one finds a very good agreement χ^{Q} and between χ^{ACCl}. This simply means that the classical description (integration over J) is not able to account for a finite contribution that comes from zero total angular momentum.

VI. RESULTS FOR TEMPERATURE-DEPENDENT RATE CONSTANTS

Temperature-dependent capture rate constants $\overline{\chi}$ are obtained from χ by averaging the latter over a Maxwell–Boltzmann velocity distribution. The distribution function F, written in terms of the variable κ, reads

$$F(\kappa;\theta)=\frac{2\theta^{-3/2}}{\sqrt{2\pi}}\kappa^2\exp\left(-\frac{\kappa^2}{2\theta}\right), \tag{27}$$

where the reduced temperature θ is given by

$$\theta=k_BT/E^*,\quad\text{with}\quad E^*=\hbar^2/\mu R_L^2. \tag{28}$$

The reduced capture rate constant $\overline{\chi}^{\mathrm{Q}}(\theta)$ is defined as

$$\overline{\chi}^{\mathrm{Q}}(\theta)=\int_0^\infty\chi^{\mathrm{Q}}(\kappa)F(\kappa,\theta)d\kappa. \tag{29}$$

Similar definitions hold for $\overline{\chi}^{\mathrm{ACQ}}(\theta)$ and $\overline{\chi}^{\mathrm{ACCl}}(\theta)$. The results of calculations are presented in Figs. 5 and 6. We see that the AC classical approximation, for $H_2(j=1)+Ar^+$ capture, performs well down to $\theta\approx 0.1$ that corresponds to 10^{-4} K. As for $\overline{\chi}^{\mathrm{ACQ}}(\theta)$, it fails in the limit of smaller θ. For $N_2(j=1)+He^+$ capture, the AC classical approximation is accurate down to $\theta\approx 1$, i.e., $T\approx 10^{-3}$ K.

Since the averaging in Eq. (29) smoothes out all fine details of the energy-dependent rate coefficient, one can try to design a simplified representation of χ^{Q}. One form, which does not require solutions of the Schrödinger equation for a complete potential but only uses the zero-energy limit of the rate coefficient for capture in an ion-induced dipole potential, reads

$$\chi_{\mathrm{app}}^{\mathrm{Q}}=\min\{\chi_0^{\mathrm{pert}},\chi^{\mathrm{ACCl}}\}. \tag{30}$$

The results for $\chi_{\mathrm{app}}^{\mathrm{Q}}=\min\{\chi_0^{\mathrm{pert}},\chi^{\mathrm{ACCl}}\}$ are obtained from Figs. 3 and 4, and lead to $\overline{\chi}_{\mathrm{app}}^{\mathrm{Q}}$ in Figs. 5 and 6.

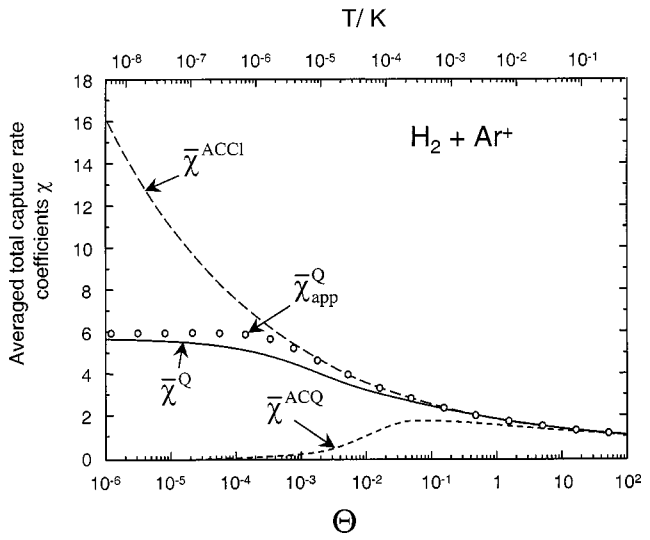

FIG. 5. $H_2(j=1)+Ar^+$ capture. Accurate quantum, $\bar{\chi}^{Q}$ (full line), adiabatic channel quantum, $\bar{\chi}^{ACQ}$ (short dashed line), and adiabatic channel classical, $\bar{\chi}^{ACCI}$ (long dashed line) reduced temperature-dependent rate constants vs scaled temperature θ (lower axis) and conventional temperature T (upper axis). Open circles correspond to $\bar{\chi}^{Q}_{app}$.

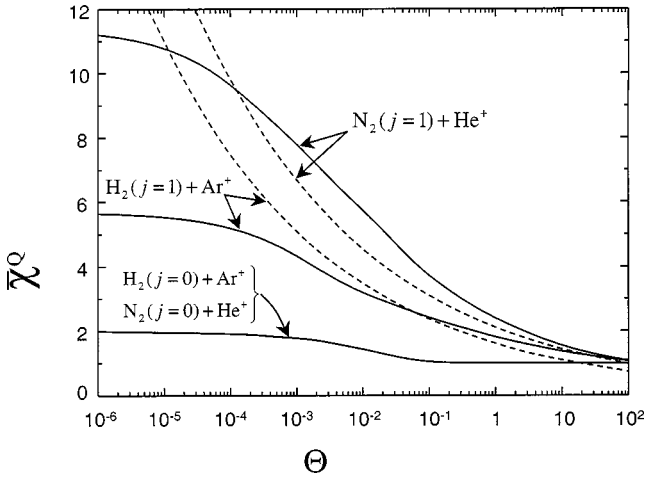

FIG. 7. Comparison of accurate reduced quantum rate constants $\bar{\chi}^{Q}$ for capture $H_2(j=0)+Ar^+$, $H_2(j=1)+Ar^+$, $N_2(j=0)+He^+$, $N_2(j=1)+He^+$ for different scaled temperatures θ. Dashed curves represent $\bar{\chi}^{ACCI}$ for pure charge–quadrupole interaction.

VII. DISCUSSION

The overall difference between capture rate coefficients for $H_2(j=1)+Ar^+$ and N_2+He^+ collisions is due to the fact that the relative role of the anisotropic interaction (ion–quadrupole) is larger for the latter case, and that the quadrupole moments of H_2 and N_2 are of different signs. For H_2 (even case), the open AC channels are those with $\omega=1$, while for N_2 (odd case) they correspond to $\omega=0$. With our normalization convention, the rate coefficients $\chi^{Q}_{H_2}(\kappa)$ and $\chi^{Q}_{N_2}(\kappa)$, for large enough κ, tend to 2/3 and 1/3, respectively. In their the zero-energy behavior, we see that, for $H_2(j=1)+Ar^+$ capture, the ratio of the zero-energy rate coefficient to the high-energy rate coefficients is about 9 while it is about 36 for $N_2(j=1)+Ar^+$ capture.

In the intermediate energy range $(2<\lambda<6)$, the quasiclassical AC rate lies between the accurate quantum and AC quantum rates. Often, quasiclassical rates at low energy are calculated by taking into account the leading term in the interaction (proportional to R^{-3}). This is permissible when the capture rate coefficient $\chi(\kappa)$ is noticeably larger than the high-energy Langevin rate coefficient χ_{Lang}. If we take a value of 3 as a value "noticeably higher than unity;" from Fig. 2 (N_2+He^+ case) we find that this value of the ratio $\chi^{N_2}(\kappa)/\chi_{Lang}$ corresponds to $\lambda\approx3$. Now, $\lambda\approx3$ is an angular momentum which is again "noticeably larger than unity," and, therefore, the small relative difference (about 15%) between the accurate and quasiclassical rates can be ascribed to the good performance of the quasiclassical approximation in the region where one can neglect the ion-induced dipole interaction against the ion–quadrupole interaction. The situation is quite different for H_2+Ar^+, see the discussion in Sec. III. A ratio $\chi^{H_2}(\kappa)/\chi_{Lang}\approx3$ is attained for $\lambda<1$. This indicates that, for H_2+Ar^+, one cannot adopt the pure ion–quadrupole interaction and, at the same time, use the classical approximation for calculation of the rate constant.

In order to illustrate the influence of the long-range ion–quadrupole interaction on the capture, in Fig. 7 we compare the capture cross sections for ground and excited states of H_2 and N_2. For both the ground and excited states the ion-induced dipole interaction is approximately the same, while the ion–quadrupole interaction is absent for nonrotating molecules. We see that the zero-temperature rate constants for rotating molecules $(j=1)$ are about 3 and 6 times higher than for the nonrotating ones $(j=0)$. Note that at $\theta=100$ the capture rate constant for nonrotating molecules has already reached its Langevin asymptote (1) while this is not the case for rotating molecules (the asymptotic values are 1/3 for N_2 and 2/3 for H_2).

If we take into account solely the ion–quadrupole interaction for $j=1$, we obtain the AC classical rate constants shown by the dashed lines in Fig. 7. These lines correspond to the formula

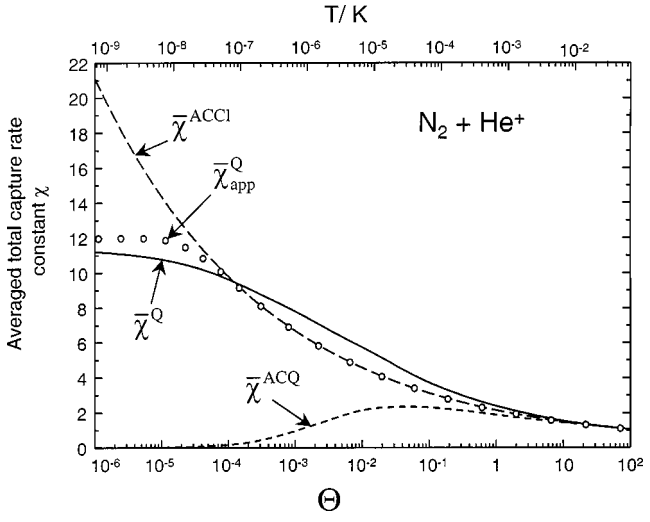

FIG. 6. As in Fig. 5 but for $N_2(j=1)+He^+$ capture.

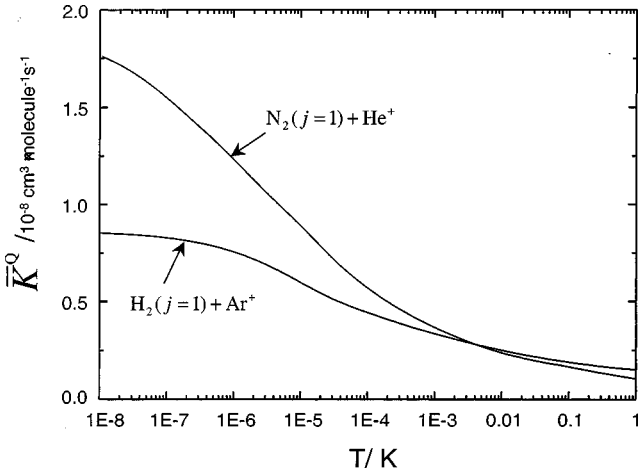

FIG. 8. Comparison of the accurate quantum rate constants $\overline{K}^{Q}$ (in $\mathrm{cm}^3\,\mathrm{s}^{-1}$) for capture events $H_2(j=1)+Ar^+$, $N_2(j=1)+He^+$ for different temperatures.

$$\overline{K}^{\mathrm{ACCl}}_{\mathrm{even}}(T)=\frac{2}{3}\Gamma(1/3)\sqrt{\frac{\pi}{\mu}}\left(\frac{k_BT}{2}\right)^{-1/6}\left|\frac{2}{5}qQ\right|^{2/3},$$
$$\overline{K}^{\mathrm{ACCl}}_{\mathrm{odd}}(T)=2^{-1/3}\overline{K}^{\mathrm{ACCl}}_{\mathrm{even}}(T) \tag{31}$$

which coincides with the results derived by Smith and Troe[4] when their expression for the state-specific limiting low temperature rate coefficients from Eq. (22) in Ref. 4 are properly weighted and $1-3a_1$ for a given ω is identified with $(2/5)\times(2-3\omega^2)$. We see once again that, at $\theta>10$ where the ACCl approximation is adequate, the ion–quadrupole model performs well for N_2+He^+ capture, while it does not for H_2+Ar^+ capture.

In order to simplify applications, finally, in Fig. 8 we present the capture rate constants in conventional units versus temperature in K.

VIII. CONCLUSION

Calculations of accurate energy-dependent rate coefficients and temperature-dependent rate constants for $H_2(j=1)+Ar^+$ and N_2+He^+ captures show two interesting dynamical features.

First, the adiabatic channel classical approximation performs well down to the energy or temperature when only a single partial rate coefficient $(J=1,\ell=0,j=1)$ essentially contributes. Here the role of the classical approximation (integration over total angular momenta and identification of the relative angular momentum with total angular momentum) is dual: it artificially simulates the quantum effects of tunneling through and reflection above the centrifugal barriers, and it suppresses too high values of centrifugal barriers such as predicted by a standard adiabatic channel approach. The former effect is similar to what has been found earlier for a single interaction potential.[1] The latter is novel, and its universality requires more studies of nonadiabatic effects in the adiabatic channel basis.

Second, a noticeable deviation of the quantum temperature-dependent rate constant from its adiabatic channel classical counterpart occurs only at extremely low temperatures (for $T<10^{-3}$ K). This property of the rate constants can be traced back to a very large range of dominance of the modified ion-induced–dipole interaction potential responsible for the *s*-wave capture. The range of dominance, R_L^M, of the modified ion-induced dipole interaction is given by $R_L^M=R_L\sqrt{1+b^2/3}$. The condition for *s*-wave capture, $k\leqslant 1/R_L^M$, is much more restrictive than the conventional condition $k\leqslant 1/R_{\mathrm{GK}}$, with R_L^M about 150 Å for the H_2+Ar^+ collisions, R_L^M about 600 Å for the N_2+Ar^+ collisions and the gas-kinetic diameter R_{GK} of the order of several Å.

On the basis of the above we thus expect that the classical version of the AC approximation will be valid also for other types of interaction down to very low temperatures such as the conditions of Bose–Einstein condensation.

ACKNOWLEDGMENTS

Financial support of this work by the Deutsche Forschungsgemeinschaft (SFB 357 "Molekulare Mechanismen Unimolekularer Prozesse") and by the KAMEO program, Israel, are gratefully acknowledged.

[1] E. I. Dashevskaya, I. Litvin, A. I. Maergoiz, E. E. Nikitin, and J. Troe, J. Chem. Phys. **118**, 7313 (2003).
[2] M. Quack and J. Troe, in *Encyclopedia of Computational Chemistry*, edited by P. V. Schleyer, N. L. Allinger, T. Clark, J. Gasteiger, and P. A. Kollmann (Wiley, Chichester, UK, 1998), Vol. 4, p. 2708.
[3] E. E. Nikitin and J. Troe, Ber. Bunsenges. Phys. Chem. **101**, 445 (1997).
[4] S. C. Smith and J. Troe, J. Chem. Phys. **97**, 5451 (1992).
[5] H. A. Bethe, Rev. Mod. Phys. **9**, 69 (1937).
[6] E. P. Wigner, Phys. Rev. **73**, 1002 (1948).
[7] E. E. Nikitin and S. Ya. Umanskii, *Theory of Slow Atomic Collisions* (Springer-Verlag, Berlin-Heidelberg, 1984).
[8] E. I. Dashevskaya, E. E. Nikitin, and J. Troe, J. Chem. Phys. **93**, 7803 (1990).
[9] E. E. Nikitin and J. Troe, J. Chem. Phys. **92**, 6594 (1990).
[10] I. I. Fabrikant and H. Hotop, Phys. Rev. A **63**, 022706 (2001).
[11] H. Hotop, M.-W. Ruf, M. Allan, and I. I. Fabrikant, Adv. At., Mol., Opt. Phys. **49**, 85 (2003).
[12] L. D. Landau and E. M. Lifshitz, *Quantum Mechanics* (Pergamon, Oxford, 1977).
[13] E. E. Nikitin and R. N. Zare, Mol. Phys. **82**, 85 (1994).
[14] A. I. Maergoiz, E. E. Nikitin, J. Troe, and V. G. Ushakov, J. Chem. Phys. **117**, 4201 (2002).